Absolute Vicarious calibration of Landsat-8 OLI and Resourcesat-2 AWiFS sensors over Rann of Kutch site in Gujarat

Shweta Sharma[a*], V. N. Sridhar[b], R.P. Prajapati[a], K. M. Rao[c] and A.K. Mathur[a]
[a]Space Applications Centre, ISRO, Ahmedabad, Gujarat, India 380015; [b]Ex-Scientist, Space Applications Centre, ISRO, Ahmedabad, Gujarat, India 380015; [c]Institute of Seismological Research, Gandhinagar, Gujarat, India
*corresponding author: shweta@sac.isro.gov.in

ABSTRACT

In this work, vicarious calibration coefficients for all the four bands (green, red, NIR and SWIR) of Resourcesat-2 AWiFS sensor for four dates during Dec 2013-Nov 2014 and for seven bands (blue, green, red, NIR, SWIR1, SWIR2 and PAN) of OLI sensor onboard Landsat-8 for six dates during Dec 2013-Feb 2015 were estimated using field measured reflectance and measured atmospheric parameters during sensor image acquisition over Rann of Kutch site in Gujarat. The top of atmosphere (TOA) at-satellite radiances for all the bands were simulated using 6S radiative transfer code with field measured reflectance, synchronous atmospheric measurements and respective sensor's spectral response functions as an input. These predicted spectral radiances were compared with the radiances from the respective sensor's image in the respective band over the calibration site. Cross-calibration between the sensors AWiFS and OLI was also attempted using near-simultaneous same day image acquisition. Effect of spectral band adjustment factor was also studied with OLI sensor taken as reference sensor. Results show that the variation in average estimated radiance ratio for the AWiFS sensor was found to be within 10% for all the bands, whereas, for OLI sensor, the variation was found to be within 6% for all the bands except green and SWIR2 for which the variation was 8% and 11% respectively higher than the 5% uncertainty of the OLI sensor specification for TOA spectral radiance. At the 1σ level, red, NIR, SWIR1 and Panchromatic bands of OLI sensor showed close agreement between sensor-measured and vicarious TOA radiance resulting no change in calibration coefficient and hence indicating no sensor degradation. Two sets of near-simultaneous SBAFs were derived from respective ground measured target reflectance profiles and applied to the AWiFS and it was observed that overall, SBAF compensation provides a significant improvement in sensor agreement. The reduction in the difference between AWiFS and OLI measured TOA reflectance was found to be within 1% for green band and within 0.5% for Red band, whereas, maximum difference was observed for NIR band (within 3.4%) after applying SBAF correction.

Keywords: Vicarious calibration, radiometric calibration, Resourcesat-2 AWiFS, SBAF, Landsat 8, 6S radiative transfer code

1. INTRODUCTION

With the advent of large number of satellites, huge amount of satellite data is available for variety of applications. Operational applications such as numerical weather prediction and climate research require accurate, well calibrated and characterized measurements with small uncertainty. The reliability of the derived data products is dependent on the proper calibration of the sensors and validation of the products. Earth Observing System (EOS) program for studying the Earth surface and atmosphere system requires variety of sensors of known radiometric stability and absolute calibration. Each of the EOS sensors is expected to maintain highly accurate calibration for its lifetime on orbit. For deriving the sensor calibration coefficients, prior to satellite launch, sensor response to illumination from a well-defined, standard source of light, traceable to well-known standards such as NIST (National Institute of Standards) is measured in the laboratory. Subsequent to satellite launch, a number of factors such as deep space environment, launch stresses etc. can affect the performance of the sensor on-board a satellite. Degradation of sensor due to these factors may lead to changes

Earth Observing Missions and Sensors: Development, Implementation, and Characterization IV, edited by Xiaoxiong J. Xiong, Saji Abraham Kuriakose, Toshiyoshi Kimura, Proc. of SPIE Vol. 9881, 98811J · © 2016 SPIE · CCC code: 0277-786X/16/$18 · doi: 10.1117/12.2227744

in calibration coefficients over time and hence, monitoring and updating the post-launch changes of sensor calibration coefficient is essential. Some satellites such as Landsat Multispectral Scanner (MSS) and Thematic Mapper (TM) use on-board lamps or solar diffusers as internal calibrators, to monitor temporal drifts in calibration coefficients. However, these are also subject to degradation over time (Thome, 2001) and therefore, it is important to have an independent method to monitor sensor calibration coefficients. Vicarious calibration provides a method to derive sensor calibration coefficients from an estimate of TOA at-satellite radiances which is completely independent from laboratory and on-board calibration. The critical elements of vicarious calibration method are selection of homogeneous test sites, properly calibrated instruments for measuring radiance of test sites and relevant atmospheric parameters and an atmospheric model to estimate at-sensor radiance. Vicarious calibration refers to the process of determining a sensor calibration coefficient using field measured surface radiance/reflectance and sensor observed DN values of the same surface, at the time of satellite pass. If the instruments used for making field measurements are traceable to NIST or other well known standards, then the vicarious calibration becomes an absolute calibration. This method has been applied to estimate vicarious post-launch calibration coefficients for Landsat Enhanced Thematic Mapper (ETM)[1-3], the Earth Observing 1 (EO-1) sensor, the Advanced Land Imager (ALI) onboard EO-1 sensor[4], Landsat-8 OLI sensor[5-6], the Advanced Wide Field Sensor (AWiFS)[7] and the Multi-angle Imaging Spectro Radiometer (MISR)[8], including estimates of uncertainties in calibration coefficients, assuming that various uncertainties are independent of each other. Biggar, Slater, and Gellman[9] discussed uncertainties in in-flight calibration of sensors with respect to ground sites. Comparison to other instruments has also been studied in the past e.g., the Landsat-7 ETM+, MODIS[10]; ASTER/VNIR and MODIS, MISR, ETM+[11], Landsat-8 OLI and Landsat-7 ETM+[12-13], IRS P6 AWiFS and Landsat sensors[14-15], Resourcesat-1 AWiFS and Landsat sensors[16]. Conventional cross-calibration is usually done by comparing band-to-band data having overlapping spectral response function. The major error sources for this type of approach are due to observation time difference, spectral response function difference in conjunction of surface reflectance and atmospheric optical depth, observation area difference[11]. Mishra et al. (2014) have studied Spectral band difference effect (SBDE) using EO-1 Hyperion images to compensate for the RSR differences between the sensors L8-OLI and L7-ETM+. Gyanesh et al. (2010)[17] used EO-1 hyperion data to calculate spectral band adjustment factors (SBAF) between the L7 ETM+ and terra MODIS sensors.

In this study, the error sources have been minimized by using near-simultaneous same day image acquisition and synchronous atmospheric measurements for AWiFS and OLI sensor of Resourcesat-2 and Landsat-8 respectively. Effect of spectral band adjustment factor was also studied with OLI sensor taken as reference sensor. Landsat-8 was launched on 11 February 2013 with two new Earth Imaging sensors to provide a continued data record with the previous Landsats. For Landsat-8, pushbroom technology was adopted, and the reflective bands and thermal bands were split into two instruments. The Operational Land Imager (OLI) is the reflective band sensor and the Thermal Infrared Sensor (TIRS), the thermal. The change from whiskbroom to pushbroom allows OLI to have a higher signal-to-noise ratio, and this is also coupled with an increase in radiometric resolution from 8 bits (ETM+) to 12 bits (OLI). The radiometric uncertainty specifications for the solar-reflective bands on OLI are ±5% (1σ) for top-of-atmosphere (TOA) spectral radiance and ±3% (1σ) for TOA spectral reflectance[18-19]. Resourcesat-2 (RS2) was launched on April 20, 2011 by ISRO with its polar satellite launch vehicle (PSLV-C16) and is a follow-on mission to Resourcesat-1 (RS1). RS2 is designed to ensure the data continuity with an enhanced radiometric resolution and improved spatial coverage[20]. The three payloads onboard include the Advanced Wide-field Sensor (AWiFS) with 56 m spatial resolution, the Linear Imaging Self-scanning Sensor (LISS3) with 23.5 m resolution, and a High resolution multispectral sensor LISS4 at 5.8 m resolution.

2. OBJECTIVES

The major objectives of the study are as follows:

1. To estimate the radiance ratio for all the seven bands of Landsat-8 OLI sensor and for all the four bands of Resourcesat-2 AWiFS sensor.

2. To study the spectral band difference effect on cross-calibration of the two sensors.

3. STUDY SITE AND DATA USED

Study area comprises of part of Rann of Kutchh as can be seen from Figure 1(a) (red box). The size of this part of Rann-of-Kutch is about 3km. x 7km, however, a smaller area has been selected with very good uniformity meeting CEOS guidelines.

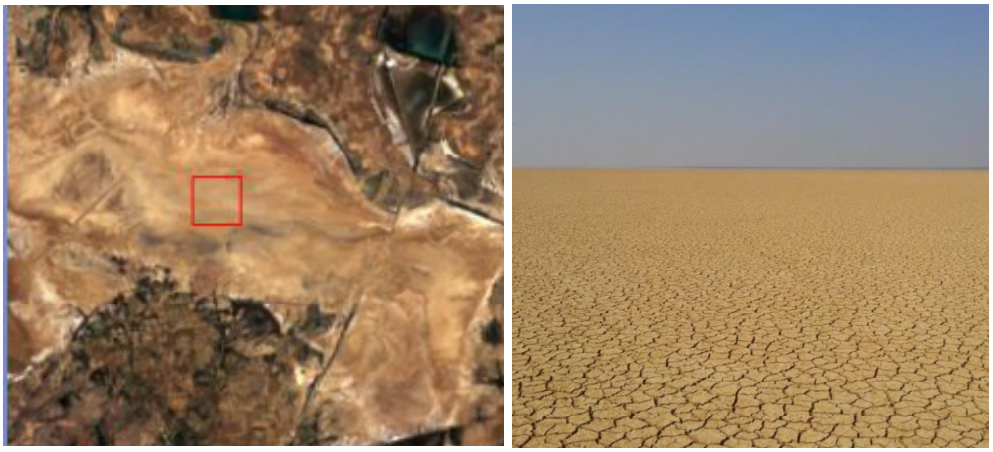

(1 a) (1 b)

Figure-1 (a): Landsat 8 image of Rann-of-Kutch site in Desalpar (b) Ground view of actual site figures.

The temporal Coefficient of Variation (CV) of the site calculated for the study period was between 5-7% for the four bands of Resourcesat-2 AWiFS sensor, indicating a high degree of temporal stability of the site. The Rann of Kutch site is an extensive mudflat which gets inundated during monsoon and flooding from fresh inland and saline water from the Gulf of Kutch during June-August. .During summer months (March – July), the Rann becomes dry and barren with high temperatures (>40 deg C), resulting in creation of salt encrusted flat wasteland, totally devoid of vegetation. Satellite data from the AWiFS sensor onboard Resourcesat-2 and OLI sensor onboard Landsat-8 were used in this study.

Table 1. Satellite data used in this study.

Satellite and Sensor	**Date of acquisition and field measurements**	**No. of ASD measurements locations**
Landsat-8 OLI sensor	03-Dec-2013	
	19-Dec-2013	
	20-Nov-2014	25
	06-Dec-2014	
	22-Dec-2014	
	08-Feb-2015	
Resourcesat-2 AWiFS sensor	19-Dec-2013	
	25-Mar-2014	25
	18-Apr-2014	
	20-Nov-2014	

Table 2. Major specifications of OLI and AWiFS sensor

System Parameter	OLI	AWiFS
Spatial Resolution (m)	OLI multispectral bands 1-7,9: 30-meters OLI panchromatic band 8: 15-meters	56 m
Swath (Km)	185	740
Altitude (km)	705	817
Quantization (bits)	12	12

Details of the data and dates of field measurements of the study site in Rann of Kutch are given in Table 1, while key specifications of the sensors and other details regarding central wavelength, saturation radiance, and pre-launch calibration coefficients are given in Table 2.

4. METHODOLOGY

The vicarious calibration is, in principle, a comparison of estimated TOA radiance with satellite measured radiance over the same ground area at the same time. Alternatively, the quantized DN sensor values are converted to radiance using pre-launch calibration coefficients, and an atmospheric correction code is applied to retrieve surface reflectance, which is then compared with field measured reflectance. Using this approach, vicarious calibration coefficients for the OCM2 (Ocean Color Monitor) sensor onboard Oceansat-2 and also the AWiFS (Advanced Wide Field Sensor) sensor onboard Resourcesat-1 has already been estimated[21]. In this study, adopting the same methodology and using the 6S code[22] in forward mode, TOA radiance for a measured field reflectance and atmospheric parameters was estimated. In the inverse mode, the surface reflectance is retrieved from TOA radiance or reflectance with the same atmospheric parameters. The simulated TOA radiance computed in the forward mode is compared with satellite measured radiance to estimate the radiance ratio. The comparison is done by comparing mean radiance with 1σ error limits. TOA at-satellite radiance is estimated using field-measured reflectance and sunphotometer atmospheric measurements for each date. The details of data analysis are as follows:

Step 1: Using ViewSpecpro software, the mean and standard deviation of the field-measured spectral reflectance (350–2500 nm) over the sampling points within the site is calculated and exported to Excel format for further computations.

Step 2: The averaged reflectance data at 1 nm interval corresponding to Resourcesat-2 AWiFS and Landsat-8 OLI bands are extracted over the full bandwidth.

Step 3: Both SRF and reflectance data are re-sampled to 2.5 nm intervals using a spline interpolation method (required by the 6S code) using MATLAB code.

Step 4: The 6S code is used to compute TOA radiance. The inputs are sun-sensor geometry (sun and view zenith and azimuth angles), atmosphere model, aerosol model, AOD, levels of ozone and water vapour, and ground reflectance.

For computing the TOA radiance, 6S code assumes US 62 standard atmosphere profile[22], it computes the extinction coefficient, single scattering albedo, asymmetry parameter, and phase function using Mie theory. The US 62 atmosphere profile gives pressure, temperature, water vapour, and ozone concentrations as a function of height (up to 100 km), at discrete intervals of 34 layers. In forward mode, the 6S code computes TOA reflectance and radiance for given surface reflectance, while in the inverse mode the code computes atmosphere-corrected surface reflectance for the same atmospheric parameters as in the forward model, for a given TOA at-satellite radiance input. Figure-2a & 2b show the Spectral Response Function of OLI sensor of Landsat-8[23] and AWiFS sensor of Resourcesat-2[24] respectively used in the present analysis. These SRFs are used to compute the spectral radiance/reflectance for each band of sensors in 6S code analysis. TOA radiance/reflectance is one of the outputs of the code. In order to estimate the radiance ratio, average radiances read from the image for OLI and AWiFS are divided by the corresponding TOA radiance estimated using 6S code.

Cross-calibration between the two sensors OLI and AWiFS was carried out using near-simultaneous image pairs, acquired during an underfly event on 19th December 2013 and 20th November 2014 along with the synchronous atmospheric parameters measurements. Due to the different spectral response of both the sensors for the respective bands, there exists a band offset when attempting the cross-calibration between these sensors. For resolving the uncertainty arising from their RSR differences, synchronous ground reflectance values were used which was measured using ASD spectro-radiometer. This compensation factor used to compensate for the spectral band differences is known as SBAF and was estimated in the present study using OLI sensor as the reference satellite sensor.

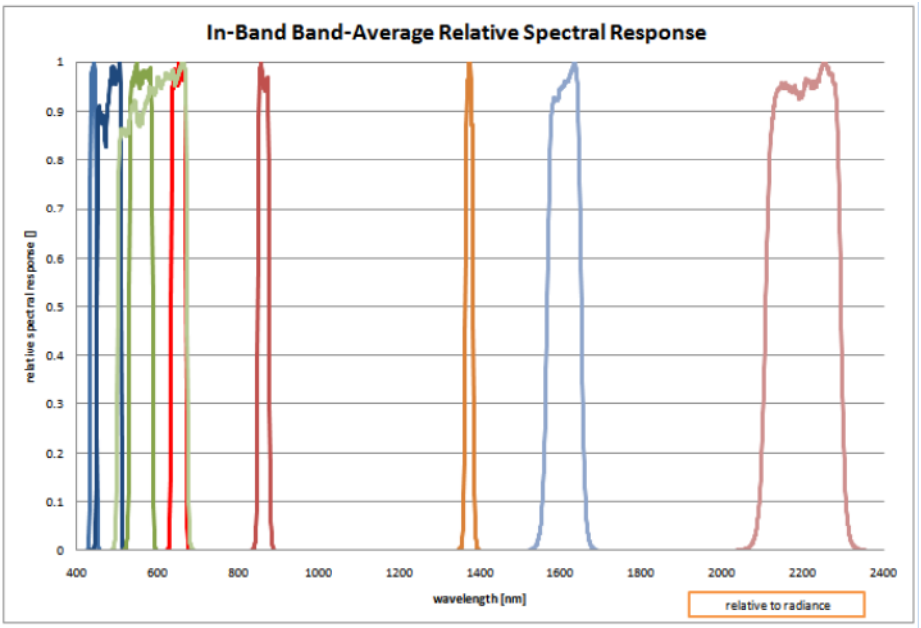

Figure 2a. Spectral Response function of OLI sensor (source: USGS site)

For the estimation of SBAF, following steps were adopted:

1. The TOA reflectance values were simulated for both the sensors (OLI and AWiFS) using the ground measured hyperspectral profile of the target, synchronous atmospheric parameters and 6S. The “simulated” TOA reflectance refers to the reflectance obtained from integrating the RSR of the multispectral sensor with the hyperspectral profile of the target.

2. By taking the ratio of the two respective simulated TOA reflectances for AWiFS and OLI sensors (with OLI sensor as a reference), SBAF was estimated for each band. The ratio of the two simulated reflectance gives a quantitative measurement of the difference factor of the two sensor spectral responses arising from different RSR for a given band and target[17, 25-26].

3. After the calculation of SBAF, AWiFS sensor's measured TOA reflectance was divided by the SBAFs to adjust for the RSR differences between the two sensors.

4. For the calculation of TOA reflectance for AWiFS sensor's image, following equation was used:

$$\rho^*(\lambda) = \frac{\pi \times L_a\,(\lambda) \times d^2}{E_0(\lambda) \times cos\theta_s} \tag{1}$$

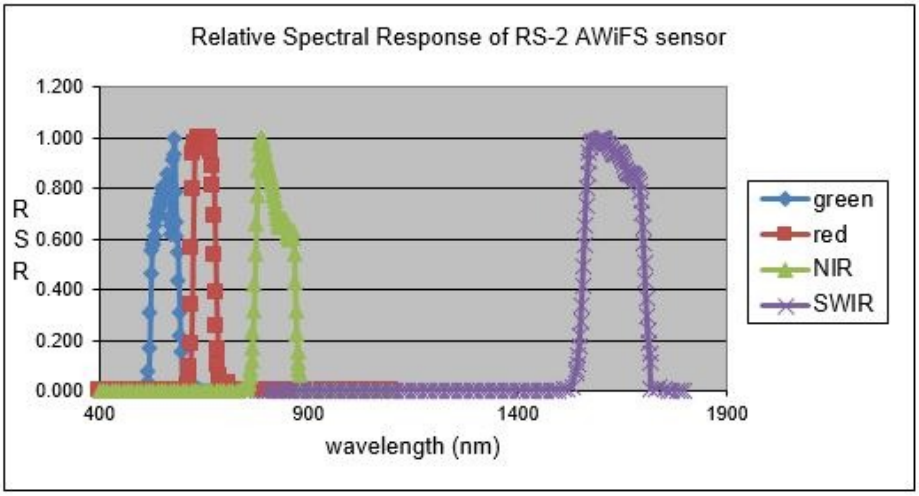

Figure 2b. Spectral Response Function of AWiFS sensor (source: Pandya and Singh, 2014)

where, d is the sun-earth distance in the Astronomical Units (AU), La(λ) is the radiance from the image for the corresponding band, E_0 is the bandpass exo-atmospheric solar irradiance for a particular spectral channel of a sensor (provided in Table 3) and θs is solar zenith angle.

Table 3. Bandpass exo-atmospheric solar irradiance (E_0, in mW/cm2/μm) values for RS2-AWiFS spectral bands[27]

Spectral band	E0
Green	185.376
Red	158.978
NIR	109.479
SWIR	23.703

5. OLI image data was converted to TOA reflectance using a conversion equation given as[12]

$$\rho\grave{}_\lambda = M_\rho \times Q_{cal} + A_\rho \quad (2)$$

where,

ρ_λ̀: TOA planetary reflectance, without correction for solar angle

Mρ: Band-specific multiplicative rescaling factor (from header file provided with the Landsat data)

Aρ: Band-specific additive rescaling factor (from header file provided with Landsat data)

Qcal: Quantized and calibrated standard product pixel values (DN)

The TOA reflectance with a correction for solar zenith angle is given as

$$\rho_\lambda = \frac{\rho\grave{}_\lambda}{\cos(\theta_{SZA})} \quad (3)$$

where, ρ_λ: TOA reflectance; θ_{SZA}: Solar Zenith angle

5. RESULTS AND DISCUSSION

Radiance ratio of satellite sensor measured average TOA radiance with mean plus and mean minus one standard deviation (μ±1σ) and estimated TOA radiance using field measurements and 6S is shown in figure 3(a) and 3(b) for all the dates of OLI and AWiFS sensor respectively.

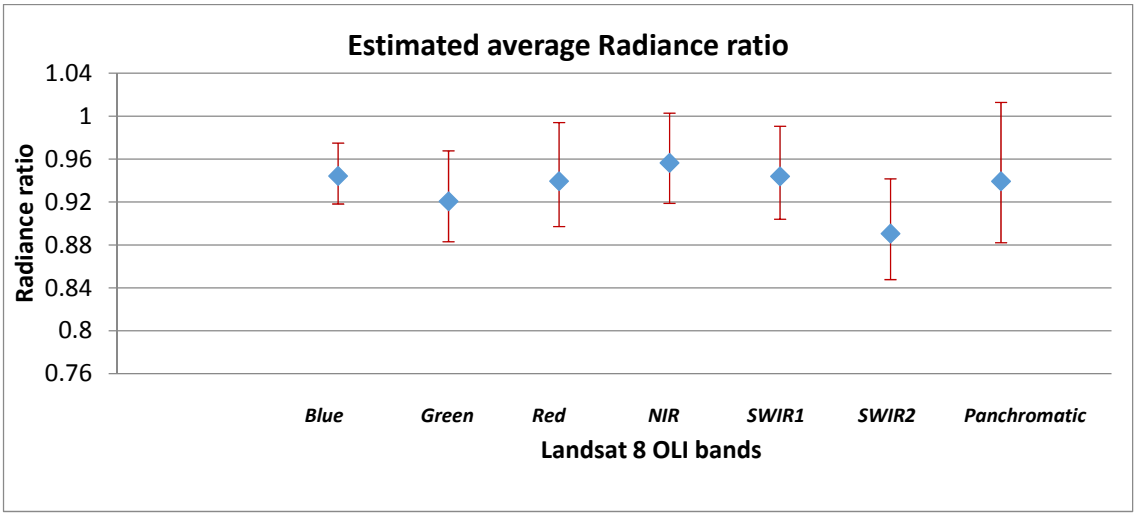

Figure 3a. Average radiance ratio for Landsat-8 OLI sensor bands

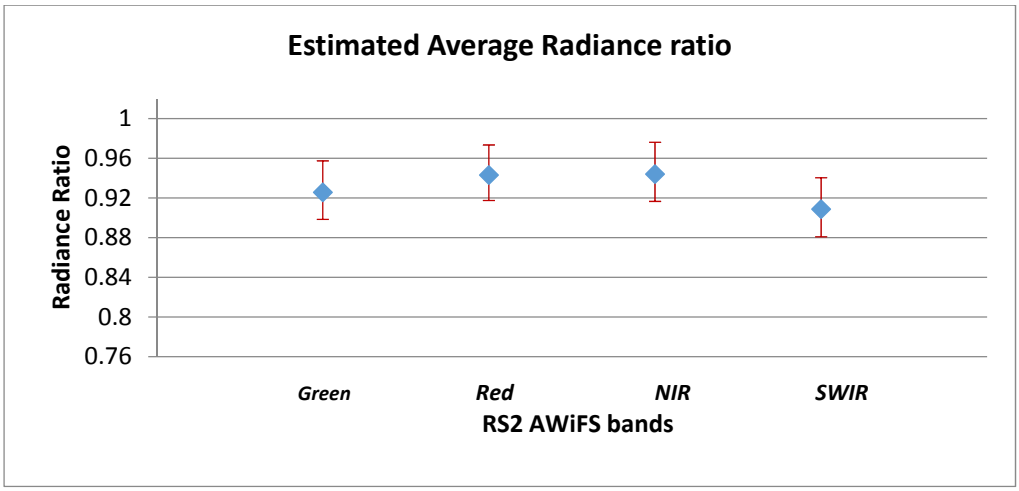

Figure 3b. Average radiance ratio for Resourcesat-2 AWiFS sensor bands (uncertainty bars are 1σ standard deviation)

It can be seen from Figure 3a that at the 1σ level, the radiance ratio for red, NIR, SWIR1 and Panchromatic bands of OLI sensor either passes through 1 or approaches unity which shows close agreement between sensor-measured and vicarious TOA radiance resulting in no change in calibration coefficient and hence indicating no sensor degradation. Whereas, for green and SWIR2 bands, the radiance ratio variation was found to be 8% and 11% respectively which are slightly higher than the 5% uncertainty of the instrument specification for TOA spectral radiance, indicating the change in calibration coefficients. The OLI is required to produce data calibrated to an uncertainty of less than 5% in terms of absolute, at-aperture spectral radiance and to an uncertainty of less than 3% in terms of top-of-atmosphere spectral reflectance for each of the spectral bands[28]. For all the bands of Resourcesat-2 AWiFS sensor, the percent difference between the sensor measured and 6S estimated TOA radiance was found to be within 10%.

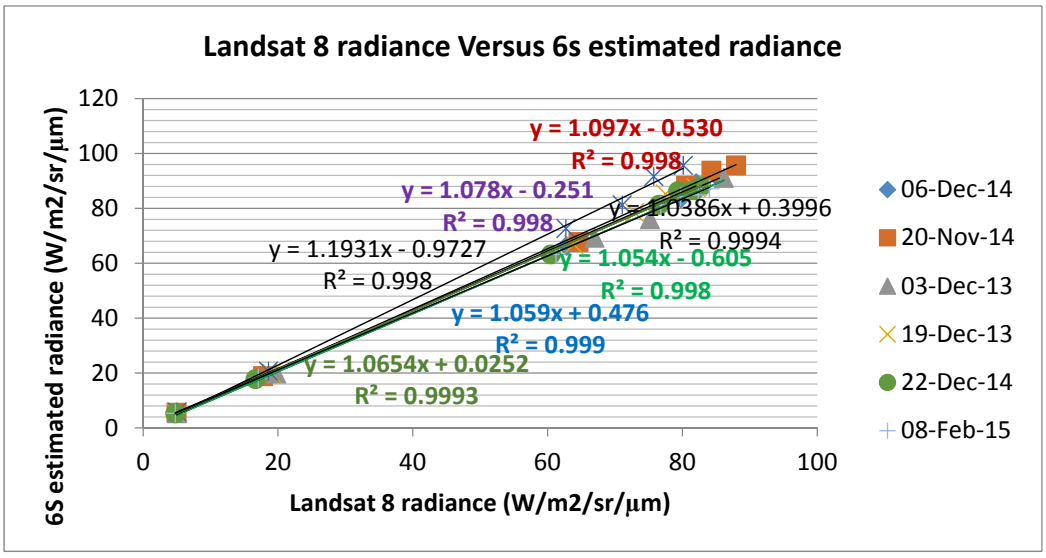

Figure 4. Average radiance ratio for Resourcesat-2 AWiFS sensor bands (uncertainty bars are 1σ standard deviation)

For the cross-comparison of the two sensors (OLI and AWiFS) Landsat-8 OLI sensor was used as reference sensor because it was observed that the OLI sensor measured TOA radiances for all the dates were in close agreement with 6S predicted TOA radiance as can be seen from Figure 4, the correlation between 6S estimated radiance and Landsat 8 radiance for all the dates is very high with R2 value being greater than 0.99. With OLI sensor as the reference, SBAF was calculated using the approach mentioned in the methodology section and using near-simultaneous image pairs for two dates 19th Dec 2013 and 20th Nov 2014. Table 4 shows the estimated SBAF for all the bands of AWiFS.

Table 4. Estimated SBAF using simulated TOA reflectances

Bands/Sensor ↓ →	**Simulated TOA reflectance for 20-Nov-14**		**SBAF for 20-Nov 14**	**Simulated TOA reflectance for 19-Dec-13**		**SBAF for 19-Dec 13**
	L8 OLI	**RS2-AWiFS**		**L8 OLI**	**RS2-AWiFS**	
Green	0.2295768	0.227591	**0.991**	0.2251242	0.223128	**0.991**
Red	0.2764173	0.275271	**0.996**	0.2733429	0.27293	**0.998**
NIR	0.316262	0.304563	**0.963**	0.335882	0.323505	**0.963**
SWIR	0.3493847	0.35066	**1.003**	0.397321	0.402469	**1.013**

Tables-5a & b show the comparison of TOA reflectance computed from the image for Landsat-8 OLI and RS2 AWiFS for Desalpar site and corresponding SBAF effect. By comparing the TOA reflectance instead of at-sensor spectral radiance, the cosine effect of different solar zenith angles due to the time difference between data acquisitions was removed. Second, TOA reflectance compensates for different values of the exo-atmospheric solar irradiance arising from spectral band differences. Third, the TOA reflectance corrects for the variation in the Earth–Sun distance between different data acquisition dates. These variations can be significant geographically and temporally.

Two sets of near-simultaneous SBAFs were derived from respective ground measured target reflectance profiles and applied to the AWiFS. It is clear from Table 5a, for band 1, before SBAF, the difference between AWiFS and OLI measured TOA reflectance was 2.36%, which was reduced to 1.48% after SBAF compensation. Similarly, the disagreement between AWiFS and OLI TOA reflectances are reduced from -4.66% to -5.08% for band 2, 11.69% to 8.30% for band 3, whereas, for band 4, it increased from 13.93% to 14.18% after applying SBAF. Similar results can be seen for 19th Dec 2013 (Table 5b) except for SWIR band where the increase is more as compared to 20th Nov 2014, SWIR band results. Overall, SBAF compensation provides a significant improvement in sensor agreement. From Tables 5 (a) and (b), it is observed that for both the dates, the reduction in the AWiFS and OLI TOA reflectance difference is within 1% for green band and within 0.5% for Red band, whereas, maximum difference was observed for NIR band (within 3.4%) after applying SBAF correction.

Table 5a. Effect of SBAF on TOA reflectance comparison of OLI and AWiFS for 20th Nov 2014

	TOA reflectance calculated from image for 20-Nov-2014			**Percent Difference between TOA reflectance d=(a-b)/a**	**Percent Difference between TOA reflectance with SBAF correction e=(a-c)/a**
Bands/Sensor	**L8 OLI (a)**	**RS2 AWiFS (b)**	**SBAF corrected RS2 AWiFS TOA reflectance (c)**		
Green	0.206319	0.20144	0.203269	**2.36**	**1.48**
Red	0.255318	0.267223	0.268296	**-4.66**	**-5.08**
NIR	0.306242	.27043	0.280820	**11.69**	**8.30**
SWIR	0.339202	.29195	0.291077	**13.93**	**4.18**

Table 5b. Effect of SBAF on TOA reflectance comparison of OLI and AWiFS for 19th Dec 2013

Bands/Sensor	TOA reflectance calculated from image for 19-Dec-2013			Percent Difference between TOA reflectance d=(a-b)/a	Percent Difference between TOA reflectance with SBAF correction e=(a-c)/a
	L8 OLI (a)	RS2 AWiFS (b)	SBAF corrected RS2 AWiFS TOA reflectance (c)		
Green	**0.197833**	**0.1623**	0.163774	17.96	17.21
Red	**0.245777**	**0.20115**	0.201553	18.15	17.99
NIR	**0.317809**	**0.26249**	0.272575	17.41	14.23
SWIR	**0.376528**	**0.3213**	0.317177	14.67	15.76

6. CONCLUSIONS

In this study, absolute vicarious calibration was carried out for all the four bands of Resourcesat-2 AWiFS sensor and for seven bands of Landsat-8 OLI sensor using the data acquired during Dec 2013-Feb 2015 over cal-val site at Desalpar, Rann of Kutch in Gujarat. Desalpar site was found to be very uniform having CV between 5-7% and very useful for performing vicarious absolute radiometric calibration of medium and coarse resolution spacecraft sensors. From the analysis, it was observed that for all the bands of Resourcesat-2 AWiFS sensor, the percent difference between the sensor measured and 6S estimated TOA radiance was within 10%, whereas, for OLI sensor, for green and SWIR2 bands, the radiance ratio variation was found to be 8% and 11% respectively which are slightly higher than the 5% uncertainty of the instrument specification for TOA spectral radiance, indicating the change in calibration coefficients for these bands. Cross-calibration between the sensors AWiFS and OLI was also attempted using near-simultaneous same day image acquisition. Effect of spectral band adjustment factor was also studied with OLI sensor taken as reference sensor. It was observed that overall; SBAF compensation provided a significant improvement in sensor agreement. The difference between AWiFS and OLI measured TOA reflectance was found to be reduced after applying SBAF correction with maximum reduction (within 3.4%) observed in NIR band.

ACKNOWLEDGMENTS

The authors would like to express their gratitude and sincere thanks to Sri Tapan Misra, Director, SAC for his guidance and encouragement during the study. It is our immense pleasure to thank Dr. B.S. Gohil, Deputy Director, EPSA for his constant support.

REFERENCES

[1] Thome, K. J., "Absolute Radiometric Calibration of Landsat 7 ETM+ Using the Reflectance Based Method." Remote Sensing of Environment 78: 27–38 (2001).

[2] De Vries, C., T. Danaher, R. Denham, P. Scarth, and S. Phinn., "An Operational Radiometric Calibration Procedure for the Landsat Sensors Based on Pseudo-Invariant Targets." Remote Sensing of Environment 107: 414–429 (2007).
[3] Markham, B. L., and D. L. Helder., "Forty Year Calibrated Record of Earth Reflected Radiance from Landsat: A Review." Remote Sensing of Environment 122: 30–40 (2012) doi:10.1016/j.rse.2011.06.026.
[4] Chander, G., B. L. Markham, and D. L. Helder., "Summary of Current Radiometric Calibration Coefficients for Landsat MSS, TM, ETM+ and EO-1 ALI Sensors." Remote Sensing of Environment 113: 893–203 (2009).
[5] Czapla-Myers J., Nikolaus Anderson, Kurtis Thome, and Stuart Biggar, "The absolute radiometric calibration of the Landsat 8 Operational Land Imager using the reflectance-based approach and the Radiometric Calibration Test Site (RadCaTS)", Proc. of SPIE Vol. 9218, 921819, (2014), doi: 10.1117/12.2063321.
[6] Czapla-Myers, J.; McCorkel, J.; Anderson, N.; Thome, K.; Biggar, S.; Helder, D.; Aaron, D.; Leigh, L.; Mishra, N., "The ground-based absolute radiometric calibration of Landsat 8 OLI", Remote Sens. 7, 600-626 (2015); doi:10.3390/rs70100600.
[7] Pagnutti, M. 2006. Initial Radiometric Calibration of the AWiFS Using Vicarious Calibration Techniques. USDA FAS/PECAD Seminar, Fairfax, Virginia, USA.
[8] Bruegge, C. J., D. J. Diner, R. A. Kahn, N. Chrien, M. C. Helmlinger, B. J. Gaitley, and W. A. Abdou., "The MISR Radiometric Calibration Process." Remote Sensing of Environment 107: 2–11 (2007).
[9] Biggar, S. F., P. N. Slater, and D. I. Gellman, "Uncertainties in In-Flight Calibration of Sensors with Reference to Ground Measured Sites in 04–1.1 μm Range." Remote Sensing of Environment 48: 245–252 (1994).
[10] Angal, A.; Xiong, X.; Choi, T.; Chander, G.; Mishra, N.; Helder, D.L., "Impact of Terra MODIS Collection 6 on long-term trending comparisons with Landsat 7 ETM+ reflective solar bands", Remote Sens. Lett., 4, 873–881 (2013).
[11] Arai K., "Comparison Among Cross, Onboard and Vicarious Calibrations for Terra/ASTER/VNIR", International Journal of Advanced Research in Artificial Intelligence, Vol. 2, No.10, 14-18 (2013).
[12] Mishra, N.; Haque, M.; Leigh, L.; Aaron, D.; Helder, D.; Markham, B., "Radiometric cross calibration of Landsat 8 Operational Land Imager (OLI) and Landsat 7 Enhanced Thematic Mapper Plus (ETM+)", Remote Sens. 6, 12619–12638 (2014); doi:10.3390/rs61212619.
[13] Flood, N., "Continuity of reflectance data between Landsat-7 ETM+ and Landsat-8 OLI, for both Top-of-Atmosphere and surface reflectance: A study in the Australian landscape", Remote Sens. 6, 7952–7970 (2014); doi:10.3390/rs6097952.
[14] Gyanesh Chander, Dennis L. Helder, Gregory L. Stensaas, Thomas R. Loveland, Brian L. Markham, James R. Irons. Evaluation and Comparison of the IRS-P6 AWiFS and the Landsat Sensors. NASA LCLUC Science Team Meeting April 20 –22 (2010).
[15] Chen Xuexia, James E. Vogelmann , Gyanesh Chander, Lei Ji, Brian Tolk, Chengquan Huang and Matthew Rollins, "Cross-sensor comparisons between Landsat 5 TM and IRS-P6 AWiFS and disturbance detection using integrated Landsat and AWiFS time-series images", International Journal of Remote Sensing Vol. 34, No. 7, 2432–2453 (2013).
[16] Goward S. N., G. Chander, M. Pagnutti, A. Marx, R. Ryan, N. Thomas, R. Tetrault. Complementarity of ResourceSat-1 AWiFS and Landsat TM/ETM+ sensors. Remote Sensing of Environment 123, 41–56 (2012).
[17] Gyanesh Chander, N. Mishra, D. L. Helder, D. Aaron, T. Choi, A. Angal and X. Xiong, "Use of EO-1 hyperion data to calculate spectral band adjustment factors (SBAF) between the L7 ETM+ and terra MODIS sensors," presented at the Int. Geoscience Remote Sensing Symp. (IGARSS), Honolulu, HI, (2010).
[18] Markham, B. L., Dabney, P. W., Murphy-Morris, J. E., Pedelty, J. A., Knight, E. J., Kvaran, G., and Barsi, J. A.,"The Landsat Data Continuity Mission Operational Land Imager (OLI) radiometric calibration."Proc. IEEE,2283-2286 (2010).
[19] Markham, B., Barsi, J., Kvaran, G., Ong, L., Kaita, E., Biggar, S., Czapla-Myers, J., Mishra, N., and Helder, D., "Landsat-8 Operational Land Imager Radiometric Calibration and Stability," Remote Sensing, 6, 12275-12308 (2014); doi:10.3390/rs61212275.
[20] Resourcesat-2 Data User's Handbook, ISRO/NRSC, December 2011, Doc. No.: NRSC:SDAPSA:NDC:DEC11:364, (2011).

[21] V.N. Sridhar, Kaushal B. Mehta, R.P. Prajapati, K.N. Babu, N.M. Suthar and A.K. Shukla, "Absolute vicarious calibration of OCM2 and AWiFS sensors using a reflectance-based method over land sites in the Rann of Kutch, Gujarat", International Journal of Remote Sensing, Vol. 34, Issue 16, 5690-5708 (2013); doi:10.1080/01431161.2013.792967.
[22] Vermote, E., D. Tanre, J. L. Deuze, M. Herman, J. J. Morcrette, and S. Y. Kotchenova., "Second Simulation of Satellite Signal in the Satellite Spectrum (6S)", 6S User Guide Version 3, University of Maryland, (2006).
[23] http://landsat.usgs.gov/instructions.php (last accessed on 15th March 2016).
[24] Pandya M.R. and Singh R.P., "Development of a Scheme for Atmospheric Correction of the Resourcesat-2 AWiFS Data", Scientific Report. SAC/EPSA/ABHG/EHD/R&D/SACRS2/SR/01/2014, (2014).
[25] Bruegge C.J., N.L. Chrien, R.R. Ando, D.J. Diner, W.A. Abdou, M.C. Helmlinger, S.H. Pilorsz, K.J. Thome, and K.J. Early, "Validation of the Multi-angle Imaging Spectroradiometer (MISR) radiometric scale," IEEE Trans. On Geosciences and Remote Sensing, 40, pp. 1477–1492 (2002).
[26] Teillet, P.M.; Fedosejevs, G.; Thome, K.J.; Barker, J.L. Impacts of spectral band difference effects on radiometric cross-calibration between satellite sensors in the solar-reflective spectral domain. Remote Sens. Environ. 2007, 110, 393–409.
[27] Pandya M.R., K. R. Murali and A. S. Kirankumar, "Quantification and comparison of spectral characteristics of sensors onboard Resourcesat-1 and Resourcesat-2 satellites", Remote Sensing Letters. Vol. 4, no. 3, 306-314 (2013).
[28] Irons, J.R., et al., The next Landsat satellite: The Landsat Data Continuity Mission, Remote Sensing of Environment (2012), doi:10.1016/j.rse.2011.08.026.